Journal of Applied Geophysics 171 (2019) 103874

Contents lists available at ScienceDirect

Journal of Applied Geophysics

journal homepage: www.elsevier.com/locate/jappgeo

Non-destructive damage analysis in Kariye (Chora) Museum as a cultural heritage building

C. Çağlar Yalçıner [a], Aydın Büyüksaraç [b,*], Yunus Can Kurban [c]

[a] Çanakkale Onsekiz Mart University, Çan Vocational College, Çanakkale TR-17400, Turkey
[b] Bitlis Eren University Engineering and Architectural Faculty, Civil Eng. Dept., Bitlis TR-13000, Turkey
[c] Eskişehir Osmangazi University, Engineering and Architectural Faculty, Geological Eng. Dept., Eskişehir TR-26480, Turkey

ARTICLE INFO

Article history:
Received 26 February 2019
Received in revised form 6 September 2019
Accepted 25 October 2019
Available online 30 October 2019

Keywords:
Kariye (Chora) Museum
GPR
Ultrasonic Pulse Velocity (UPV)
Geophysics
Non-destructive testing

ABSTRACT

Non-destructive testing methods are being increasingly used in the evaluation of cultural heritage buildings. Combined geophysical methods especially can be applied to structural evaluations of these kinds of buildings. Ultrasonic Pulse Velocity (UPV) Test and Ground Penetrating Radar (GPR) were used in a complementary way as non-destructive testing techniques in this study. The main aim of the study is to analyze the internal structural configuration as well as the quality of the stone, internal geometry and physical properties of some structural elements. It was determined that the main cracks in all walls within the building are on an axis. The cracks on this crack axis were determined to have been filled during previous repairs on the GPR profiles. However, the filling material is different from the building materials that constitute the building walls and at the same time the presence of void spaces was determined.

1. Introduction

The aim of this study is to evaluate the damage to surfaces in monumental structures with GPR measurements and determine water content distribution. The damage distribution is consistent with the water content distribution. Cases examined show that the distribution of the damage can be distinguished on GPR measurements and there is a relationship between some physical properties such as amplitude, frequency, and the distribution of damage. Chora Church was originally built south of the Golden Horn at the beginning of the 5th century as part of a monastery complex outside the walls of Constantinople, and stood outside the 4th century walls of Constantine the Great. The full name of the church is the Church of the Holy Savior in the country (Fig. 1).

The name of the church carried symbolic meaning because the mosaics in the narthex section of the church represented the living places of Christ and Mary. Most of the existing structure collapsed in the early 12th century between the years 1077–1081, probably due to an earthquake. Although the church was rebuilt, it was understood that the building reached its present appearance two centuries later. Theodore Metochites, a powerful Byzantine statesman, donated many of the beautiful mosaics and frescoes to the church. It is known that Theodore's impressive decoration inside the church was completed between 1315 and 1321. The mosaic work in the church is the best example of the Palaeologian Renaissance (Van Millingen, 1912).

Atik Ali Pasha, who was the Grand Vizier of Sultan Bayezid II, ordered the Chora Church to be transformed into a mosque to be called the Kariye Mosque fifty years after Istanbul was conquered by the Ottomans. Mosaics and frescoes were covered with a layer of plaster because of the prohibition of iconic images in the Islamic faith. This covering and the frequent earthquakes in the region had a negative impact on the artwork (Ousterhout, 2002).

The building lost its function in 1948 due to a restoration program supported by the American Byzantine Institute and the Dumbarton Oaks Byzantine Studies Center. The Chora Museum was opened to visitors as a museum in 1958. Visual inspections of this building indicate structural problems in most of the arches and cracks are visible in columns, buttresses and walls. The correct study of cultural heritage structures requires the application of unified techniques, historical and structural knowledge. The restoration and reinforcement of a historical building is based on the identification of deterioration and instability factors. Climatic conditions and soil problems such as underground water, micro earthquakes etc. affect the structures through time. This is why many historical buildings with monumental characteristics need maintenance or restoration. Investigation of historical buildings using non-destructive methods is important and becoming more common. In some cases, non-destructive diagnostics can also reveal new historical details covered by old restorations, etc. On the other hand, non-destructive investigation techniques can ensure the calculation of

* Corresponding author.
E-mail address: absarac@comu.edu.tr (A. Büyüksaraç).

https://doi.org/10.1016/j.jappgeo.2019.103874
0926-9851/

Fig. 1. Kariye (Chora) Museum. (a) Location of the museum on Turkey map (red dot). (b) Ancient photo from 14th century. (c) Perspective view of the museum. (For interpretation of the references to colour in this figure legend, the reader is referred to the web version of this article.)

a restoration budget and bring economic value. Many non-destructive techniques may be acceptable for diagnostics of historical buildings.

Two methods were used to examine the deterioration of pillars of the building. For two of the columns examined, direct information about the wall structure was provided by endoscopic examination of a hole in the space behind the coating. When compared with the data obtained from direct examinations and the results obtained with non-widespread and indirect investigations; 1) It proves the great effectiveness of the two diagnostic methods used in an integrated manner to detect cracks and homogeneity in the internal structure of the structural elements. 2) It helped interpretation of the radargrams, thus providing useful information for the diagnosis of the monument. Finally, the results obtained with a standard procedure and an inverse scattering algorithm for GPR prospection were compared.

Within the scope of the studies initiated for the restoration of the Kariye (Chora) Museum, different geophysical studies were planned in and around the building to determine the scope of the restoration. Studies were examined in two parts, inside and outside the museum.

Geophysical methods were implemented, tested and approved as tools for diagnosis or monitoring of artworks or historical buildings. They are non-destructive and can monitor the internal structure of the studied environment (Martinho and Dionísio, 2014).

The expectation was that the following problems would be illuminated by geophysical studies:

- Determination of the factors affecting the basic structure of the building
- Determination of the condition of the structure, the repairs made and interventions, and the existence of the partial spaces remaining around material filled into the determined crack structure
- Investigation of marble back falls, investigation of the system of blanks
- Moisture examination behind mosaics and frescoes, investigation of swelling observed on the surface based on humidity
- Examination of the condition of the drainage system in the building
- Determination of possible water content behind the wall intended to protect the building's garden outside the building
- Identification of possible grave sites in the building
- Investigation of the condition of post-tensioning bars for building protection

2. Methodology

Indoor and outdoor geophysical prospecting surveys are increasingly used in non-destructive evaluations of structures. Especially integrated methods can be applied for the evaluation of cultural heritage buildings. We propose the use of two non-destructive testing techniques, ground-penetrating radar (GPR) and ultrasonic prospection, in this study.

2.1. Ground penetrating radar method

The GPR technique is known to have the main advantage of allowing high resolution of up to ten centimeters from a centimeter. Generally, techniques with sonic origin do not allow for a similar resolution image. The Ground Penetrating Radar (GPR) system is based on the collection of information from underground with electromagnetic frequencies. The design of the GPR system has a wide range and is

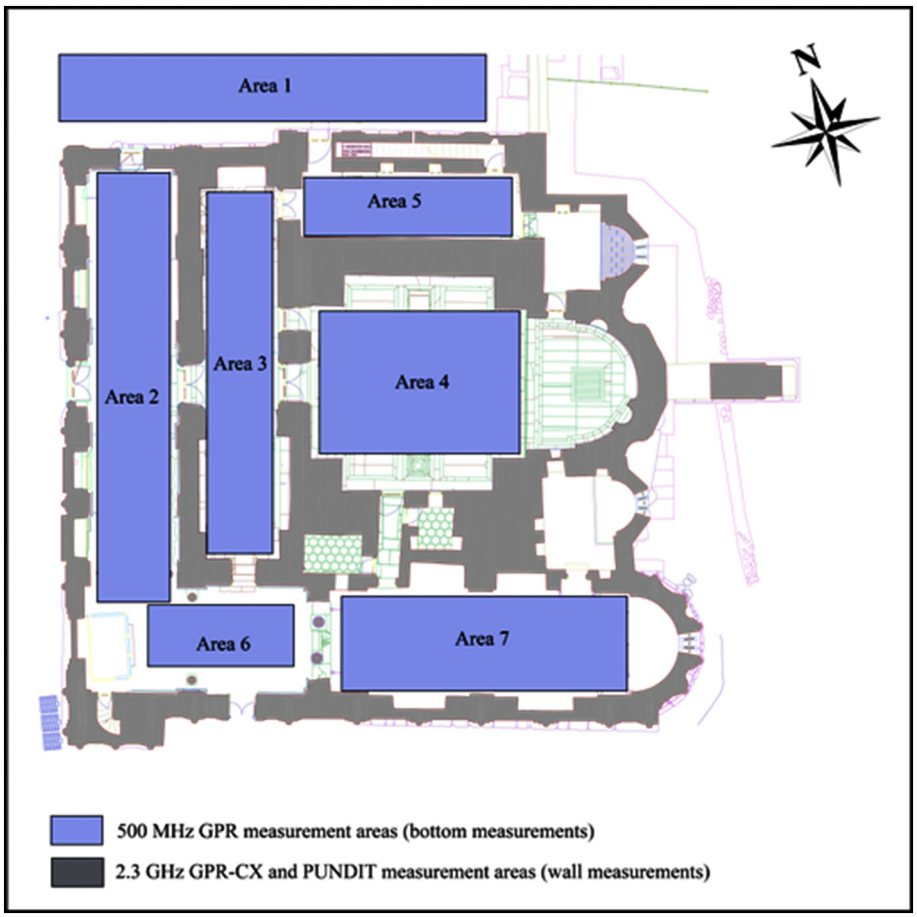

Fig. 2. Kariye (Chora) Museum measurement plan (light blue areas represent surface scans and gray areas represent wall studies with GPR-CX and UPV). (For interpretation of the references to colour in this figure legend, the reader is referred to the web version of this article.)

generally based on the selection of freely available antennas for the application to be performed. The target depth, target size and the area to be surveyed are effective in the selection process. This is quite extensive with systems available to ensure the GPR method can be selected correctly for the area of use. The ground-penetrating radar (GPR) technique is increasingly used for characterizing and monitoring the surface and subsurface of historical buildings (e.g., graves, walls, roads, structural deterioration) (Vaughan, 1986; Goodman, 1994; Goodman et al., 1995; McCann, 1995; Hruska and Fuchs, 1999; Dabas et al., 2000; Piro et al., 2000; Leckebusch, 2003; Chianese et al., 2004; Persson and Olofsson, 2004; Leucci and Negri, 2006; Leckebusch et al., 2008; Yalçıner et al., 2009; Yalçıner, 2013; Kanli et al., 2015; Barraca et al., 2016; Yalçıner et al., 2017; Buyuksarac et al., 2018). GPR consists of transmitter and receiver in antennas. Transmitting antennas emit short high frequency radio signals. GPR is generally compared to seismic reflection. GPR produces reflections from both strata and buried objects, while seismic waves only form reflections with layers.

Objects with different electromagnetic properties such as buried tanks, sedimentary layers, water table, or archaeological remains cause reflections in GPR. Generally, GPR reflections occur due to the embedded dielectric having different dielectric constants. The dielectric constant generally refers to the load that a material can store when an electromagnetic load is applied and is calculated by the formula $\varepsilon r = (c/\upsilon)^2$. Here, "εr" is the dielectric constant, "c" is the speed of light (30 cm/ns), and "v" is the transit speed of the electromagnetic energy. For this reason, the dielectric constant is inversely proportional to the electromagnetic speed. The environment in which the electromagnetic signal travels and the signal scattering are the most important elements. Two important components of energy transfer are electrical and

Fig. 3. Study photos. (a) GPR ProEx System with 500 MHz antenna. (b) GPR-CX system with 2.3 GHz antenna. (c) UPV measurement.

Table 1
Acquisition parameters of the GPR survey.

	GPR-CX	GPR
Antenna frequency	2.3 GHz	500 MHz
Trace interval	0.5 cm	1 cm
Samples	312	646
Sampling frequency	23,966.33 MHz	5862 MHz
Time window	13.018 ns	87.34 ns
Profile interval	10 cm	50 cm

Table 2
Filter processing steps and parameters of the GPR survey.

	GPR-CX	GPR
Antenna frequency	2.3 GHz	500 MHz
Time-zero correction	−1.35 ns	−4.5 ns
Subtract-mean (dewow)	0.4347 ns	2 ns
Band-pass filter	920/1840/2760/3680 MHz	200/400/600/800 MHz
Energy decay	0.512	0.512
Subtracting average	31 trace/0 to 11.6413 ns	31 trace/0 to 82.7352 ns
Velocity analysis	13 cm·ns^{-1}	10 cm· ns^{-1}
Diffraction stack migration	11 trace/13 cm·ns^{-1}/0 to 11.6413 ns/εr = 8.7	11 trace/10 cm·ns^{-1}/0 to 82.7352 ns/εr = 9

magnetic constants. Independently reflected waves (also called wave forms) are digitally collected by reflections from underground, so that many traces are gathered together and profiled as a two-dimensional vertical section. Due to the large number of reflections obtained together with the profiles in the grid, a 3D underground image can be obtained if necessary (Conyers, 2006; Yalçıner, 2013).

2.2. Ultrasonic test measurements

In order to dynamically determine the mechanical properties of the building materials in the laboratory, an ultrasonic method was developed based on the principle of obtaining wave velocities from the propagation times of seismic waves generated by transmitting a high-speed sound wave into the instrument sample. In the ultrasonic test meter, high frequency sound waves are used to measure the physical and geometrical properties of the material. These high-frequency sound waves pass through different materials at different speeds and travel through the material and then back out from the surface.

The sound waves from the ultrasonic testing device and the sound wave from the transmitter that moves on the concrete reach the receiver. The sound waves produced by the device are obtained by dividing the speed of passage through the concrete, the length of the sample, and the transit time. Ultrasonic velocity values are higher in solid bodies and lower in hollow bodies. The compressive strength of concrete varies

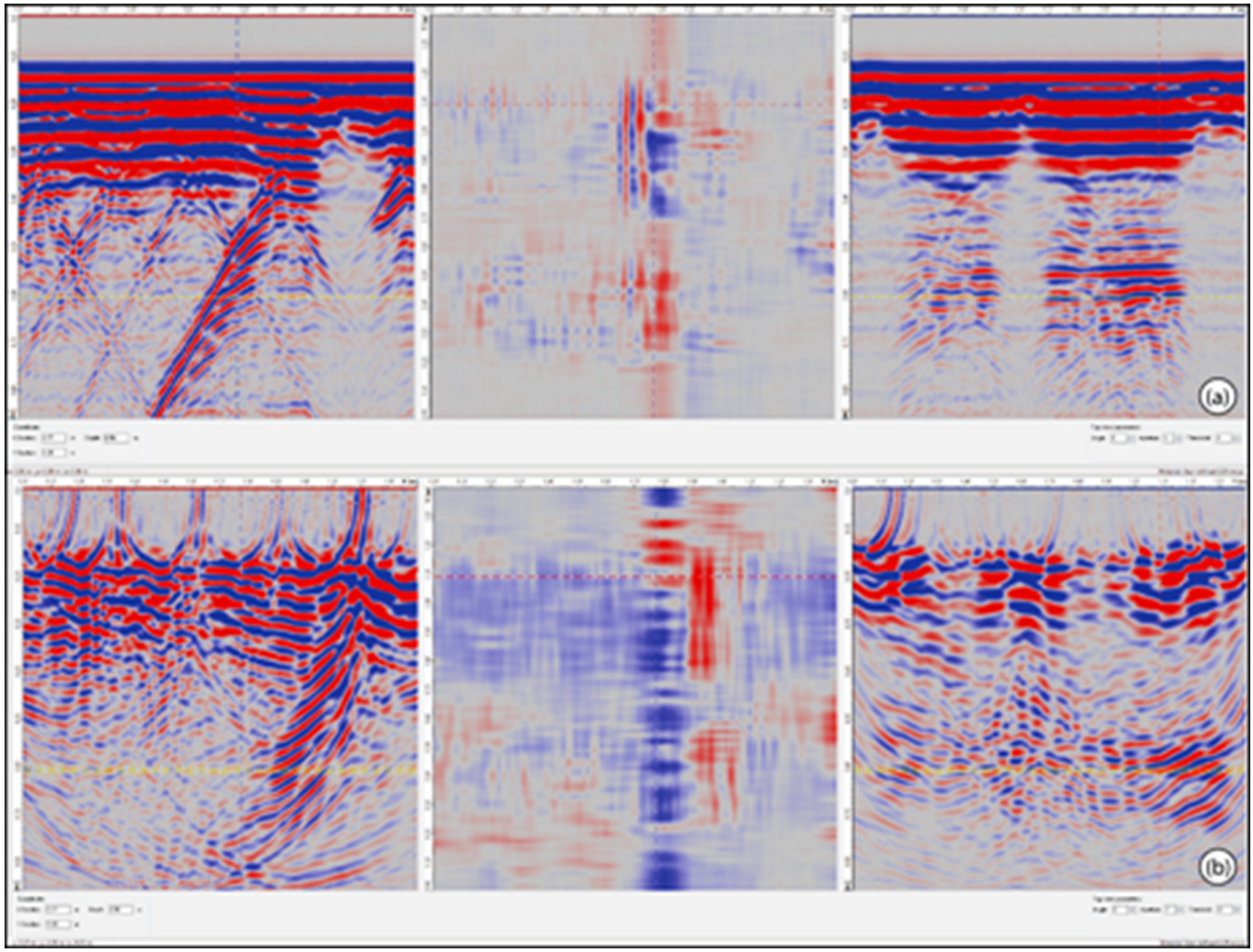

Fig. 4. Sample GPR-CX data. (a) Unprocessed data. (b) Processed data.

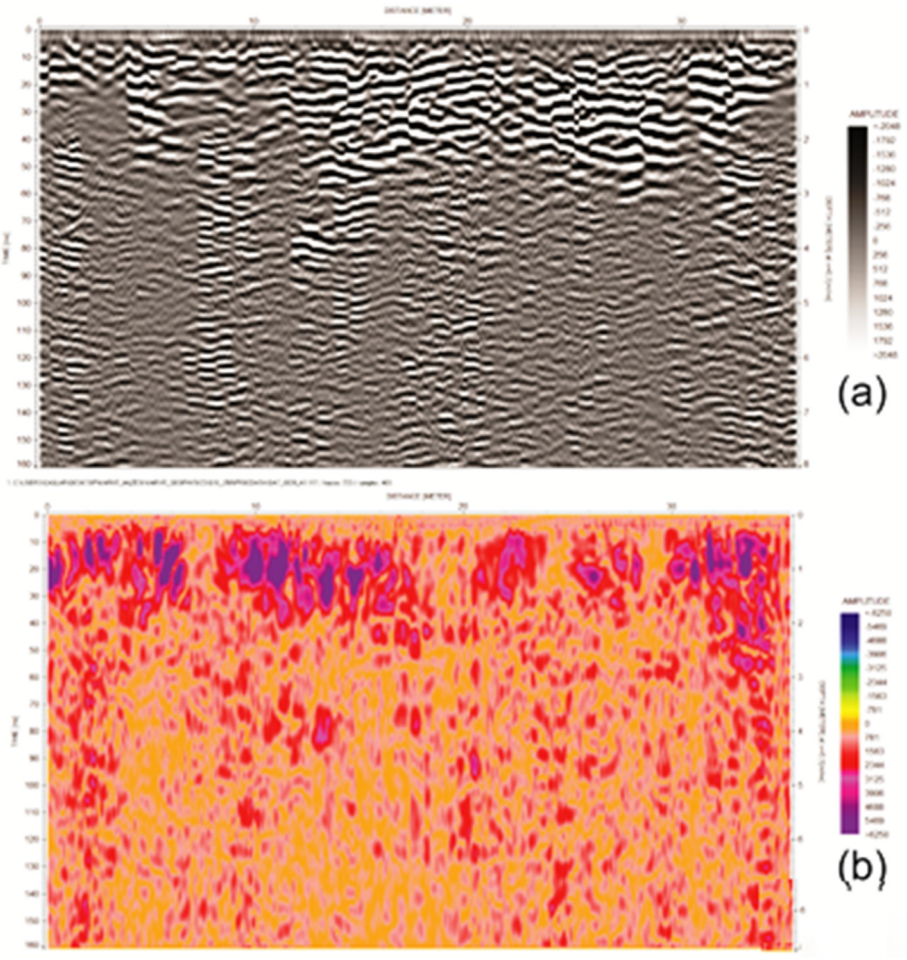

Fig. 5. Sample GPR data. (a) Processed data. (b) Post processed data with complex trace analysis.

depending on the amount of cavities in the concrete. Concrete with high sound wave transition speed has higher strength. When the receiver and transmitter are located at appropriate locations on the surface of the sample, the measurement is obtained when the pulse is first detected by the receiver from the transmitter. The device used is a portable ultrasonic undamaged digital indicator test device. The MATEST device, which is microprocessor controlled and can measure the transit time and speed through the material of the ultrasonic waveguide, can measure at 0–9999.9 microsecond time interval and 24–220 kHz. The device measures the transit time in the material between the receiver and the transmitter by bringing it into the low-frequency ultrasonic pulse field. This equipment is specially designed to find defects and failures inside materials such as concrete and steel. The equipment consists of a transmitter probe that provides sound vibration, a receiver probe that picks up the sound waves emitted by this transmitter probe, and a main body that digitally measures the time it takes to reach the receiver.

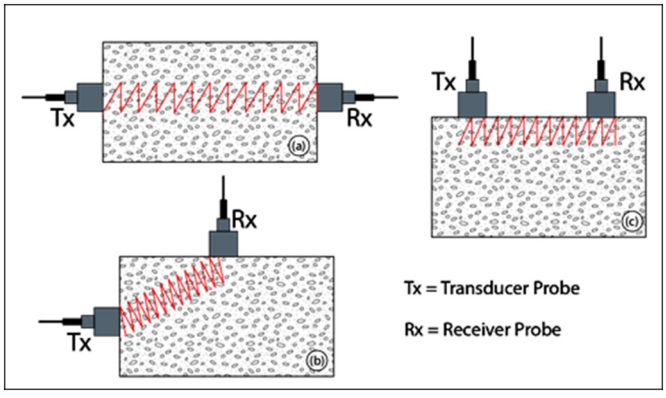

Fig. 6. UPV measuring systems. (a) Direct measurement method. (b) Semi direct measurement method. (c) Indirect measurement method.

3. Chora Museum site studies

An integrated diagnostic approach based on the use of Ground Penetrating Radar (GPR) and ultra-sonic prospecting was applied to the Kariye (Chora) Museum in Istanbul (Turkey) in this study to detect moisture, characterize the materials, and determine instability problems, cavities and structural continuity of the material in the walls and widespread deterioration of building materials (Fig. 2).

3.1. GPR studies of Chora Museum

In current buildings, radar antennas which operate with high frequency are used especially for detecting the location of objects in the carrier elements. High-frequency antennas can display very shallow effects with very high resolution. For this purpose, a MALA CX (Concrete Exploration) Monitor and “Structure Radar” device with 2.3 GHz frequency antenna was used. The device is designed so that

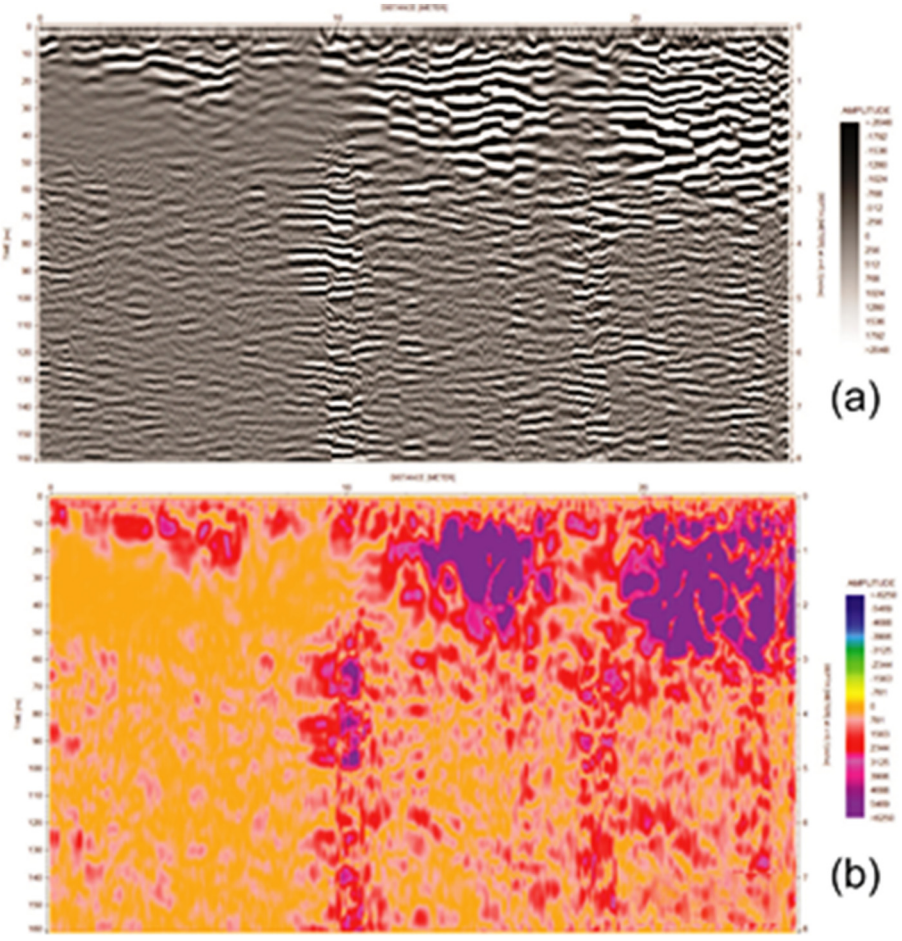

Fig. 7. 500 MHz GPR profile. (a) Processed data (black and white changes indicate wet zone). (b) Post processed data with complex trace analysis (dark blue areas indicate wet zone). (For interpretation of the references to colour in this figure legend, the reader is referred to the web version of this article.)

a structure can be explored and displayed using non-destructive methods (Fig. 3). In-wall imaging of structural walls or structural system elements, as well as the depth of irregularities such as cracks and cavities that can be identified can be illustrated by radar measurements. We also used a 500 MHz shielded GPR system around the museum to determine the environmental effects damaging the building (Fig. 3).

3.1.1. Data collection (GPR measurements)

In general, shielded antennas are used for measurements. The transmitter Tx and the receiver Rx antennas are placed to collect various marks from the underground in a box on the surface and come together to form a profile. The measurements are taken on a profile at predetermined measuring points. The radar cross-sections are obtained by adding the tracks at each measurement point side by side. When working in an area, measurements are taken using parallel profiles on the ground. Results can be displayed in three dimensions (Kadıoğlu, 2003). Reflection profiles are collected by moving the antennas along a line. Fiberglass cables and many freestanding antennas connected electronically are used for data collection. Signals collected from fiberglass cables come to the control unit and are digitized. Information from this control unit is transferred to the computer environment with various connection methods.

In this study the GPR-CX measurements were conducted by using 2.3 GHz antenna within a grid (10 cm between the profiles in both directions vertical and horizontal) (Fig. 3b). The GPR measurements used 500 MHz shielded antenna with parallel profile lines (Fig. 3a). Both measurement parameters are given in Table 1.

3.1.2. Data processing (GPR measurements)

Data processing for GPR is based on rendering the resulting numerical data into understandable images. This usually involves the use of pre-applied sample filters and process steps.

According to Danniels (2004), this is defined as reduction of data processing noise. Logically, the noise ratio in the signal causes the target to be detected. GPR usually produces too many signals contaminated with noise. The noises that can be cleaned must be filtered in the most accurate way. The algorithms for filters used to clean the noise are often very complicated. Using the most appropriate filter parameters, the original data will be minimally damaged.

After careful measurements, proper filtering appropriate for interpretation is required to produce good data (Yalçıner et al., 2009). A commercially available ReflexW (Sandmeier, 2003) program was used for these procedures (Table 2). The main process steps can be summarized in the MALÅ GPR CX System software also allows mapping of objects along 2D and 3D grids (Fig. 4). The system is entirely designed to operate with very high frequency antenna systems. Within the scope of the project, 2 antennas with 2 different frequencies were used.

One was a 500 MHz antenna (Fig. 5) which provides medium penetration with high frequency antennas. On the other hand, the 2.3 GHz antenna can measure with very high precision.

3.2. Ultrasonic test measurements on walls

The speed of the ultrasonic impact in a solid depends on the elastic properties and density of the material. The quality of some materials

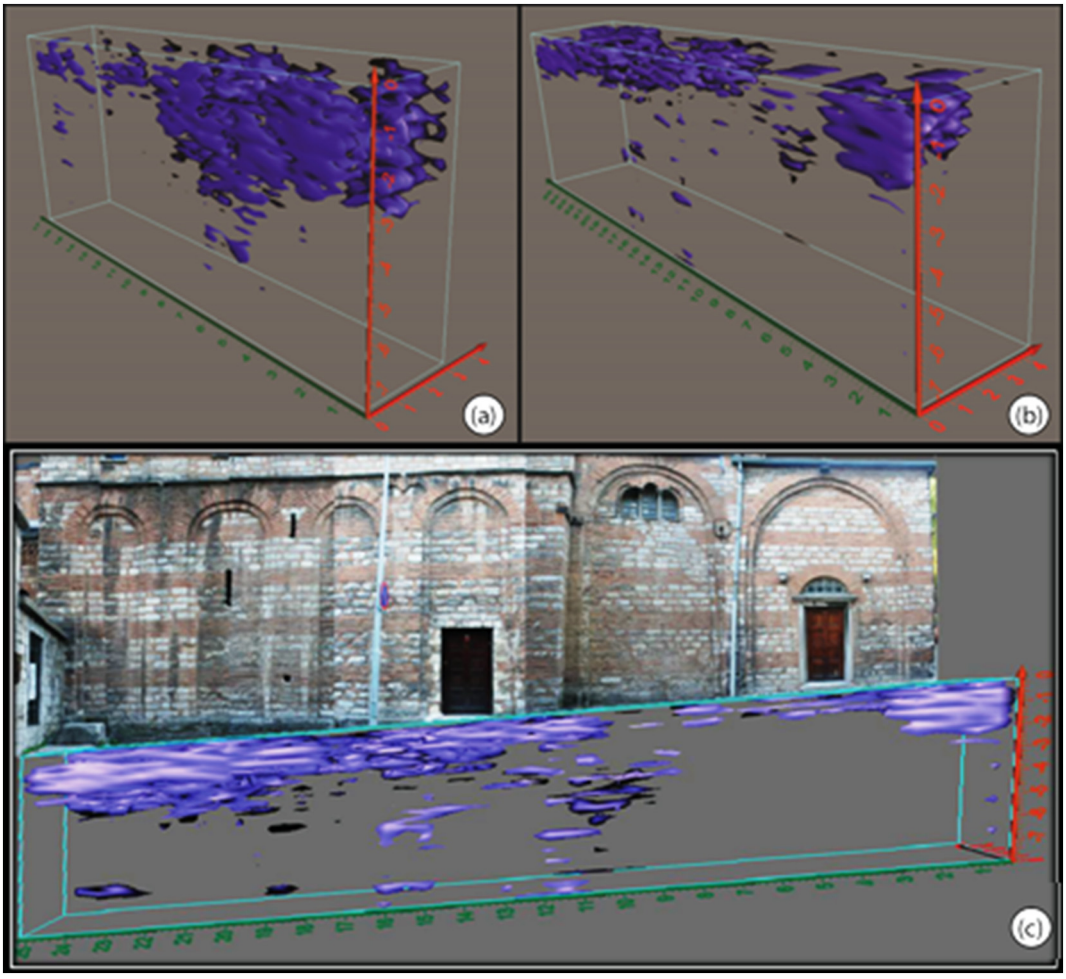

Fig. 8. 3D volumetric cube illustration of GPR data. (a) First part of the volumetric cube. (b) Second part of the volumetric cube. (c) Volumetric cube model placed on the photo in front of the museum entrance door.

varies depending on the elastic stiffness. Therefore, the ultrasonic pulse rate measuring device is often used to determine the quality of the material as well as the elastic properties. The quality of concrete and wood materials, apart from metal, can be measured in this way. When ultrasonic testing is applied to metals, internal cracks in these materials allow reflection in the radial direction and detection by collection of these signals by the receiving probe. The device can be positioned several times for crack propagation on the surface, and the crack position can be estimated as much as possible. Measurements are taken in 3 forms; direct, semi-direct and indirect. In direct measurements, the receiver and transmitter of the device are held mutually. The technique gives more reliable results than other measurement techniques because the maximum energetic longitudinal waves emitted from the transmitter are perpendicular to the receiver surface. This measurement technique cannot always be used for in situ studies (Fig. 6a). In semi-direct measurements, the angle between the receiver and transmitter ends is 90°. The technique is moderately sensitive compared to the other two transmission techniques. Despite successful use of this measurement technique, some errors may occur in the accuracy of the signal length measurements (Fig. 6b). In the non-direct measurement method, the transmitter and receiver ends are placed on the same surface and ultrasonic speed is provided by the distance between the centers of the transmitter and receiver ends. When this method is used, the impact detected by the direct method on the same path length is reduced by 1–2%. The direct measurement method is based on the principle of taking measurements at various distances from the surface of homogeneous regions. The transition time values obtained in this way can be used as if measured directly by applying the correction factor (Fig. 6c).

The ultrasonic speed method is used to determine the damage due to environmental conditions in the building, to determine the internal structural damage in the cracks and after freeze-thaw events. It is also used to identify cracks and voids. Dynamic elastic parameters such as elastic modulus, shear modulus and Poisson's ratio for rocks can be calculated at ultrasonic speeds. Frequencies commonly used for investigating non-metallic materials are 50–100 kHz. The ultrasonic speed method is a cheap and practical method for testing concrete pressure resistance. It is used very successfully in the process of finding segregations and discontinuities in building elements.

3.3. Results

GPR, GPR-CX and UPV measurements were carried out on the walls of the museum, floor of the museum and around the museum with the aim of detecting underground water near the museum. In these studies, it was determined that underground water is very close to the museum base and that these waters are effective up to about 3 m depth.

3.3.1. GPR results

The obtained 2D cross-sections (Fig. 7) were transformed into 3D images with the help of interpolation (Fig. 8). In order to make the study more understandable, the accumulation of underground water in front of the side entrance gate is shown in Fig. 8 with 3-dimensional model dressing.

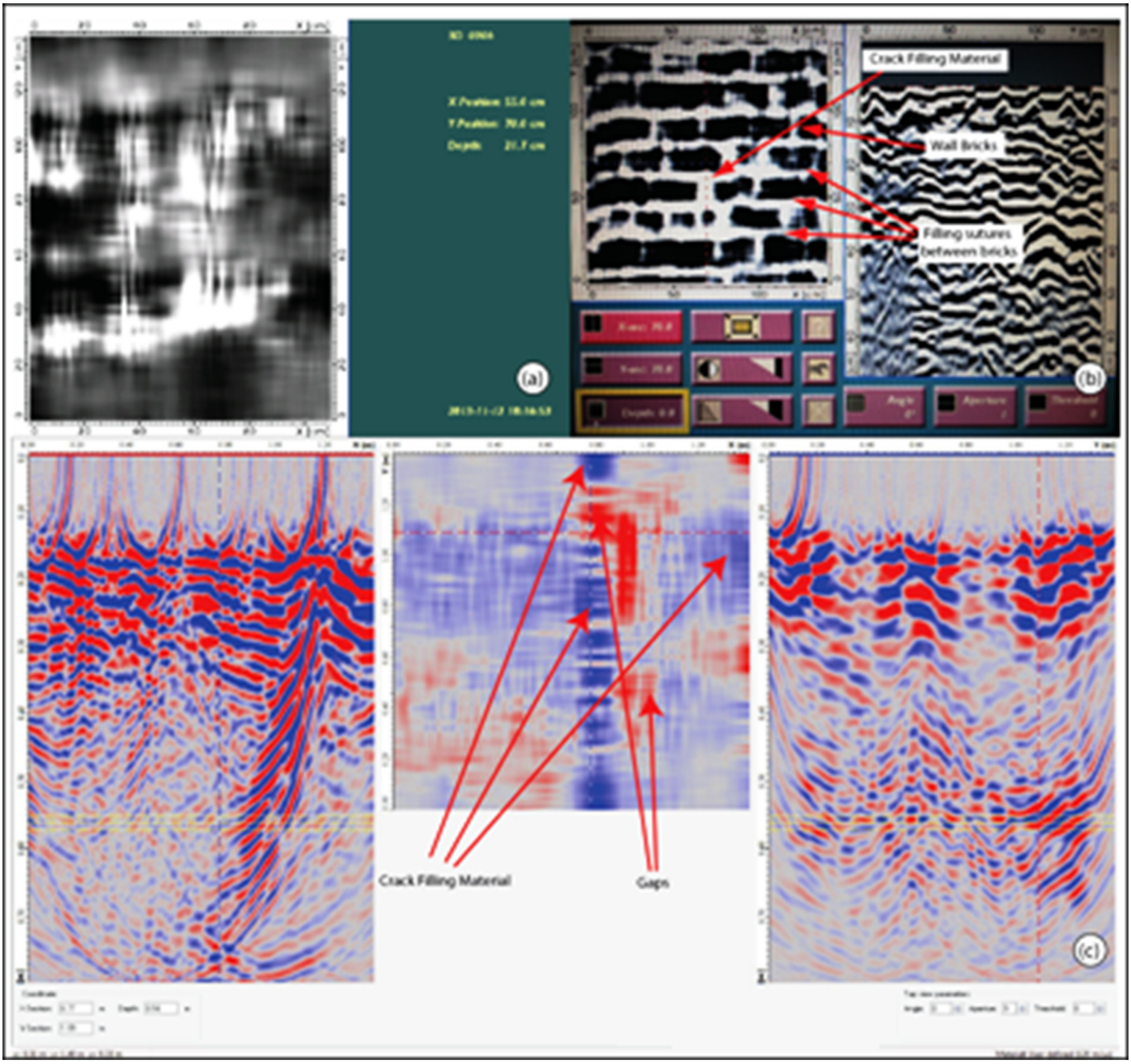

Fig. 9. GPR-CX 3D visualization. (a) The raw data from GPR-CX equipment (white areas represent gaps). (b) Processed data from GPR-CX equipment. (c) The 3D vision software result after processing.

Findings obtained around the museum building found a direct impact of underground water, and the floor on which the foundation rested was also very influential. In particular, the area where the entrance is located in the north-northeast part of the museum building (Fig. 8) appears to be the area most affected by underground water. For the drainage system to be effective in this area, it is necessary to improve the existing floor (base circumference) and construct a proper drainage system. The fissures formed on the museum building are thought to be the problem and foundation of the primary cause. It is also necessary to intervene by improvement of the foundation during drainage.

The channels and busses, which are affected by the problem identified and which are frequently seen around the museum building, should be moved as far as possible away from the building.

The backyard, which is the place where the topographic slope and surface and underground waters collect, especially problems described with the upper stories and visually in Fig. 7, is directly affected by the geological construction under the backyard. For this reason, it is very important to determine whether the system is examined or not or if there is detailed examination of the set located between the museum and the park to the south-east of the museum.

3.3.2. GPR-CX results

The irregularity of the spaces found behind the marbles, especially those covered by the naos walls (Fig. 9), indicates that such spaces were not made for an objective purpose (channel style). It is necessary to intervene in these spaces which are quite wide. The gray shades represent different materials on in-wall images resulting from GPR-CX (Fig. 9b).

Moisture is observed in mosaic and fresco-covered walls which are not covered with marble. On some walls, swelling was also detected in addition to this humidity. Restoration will reduce this effect.

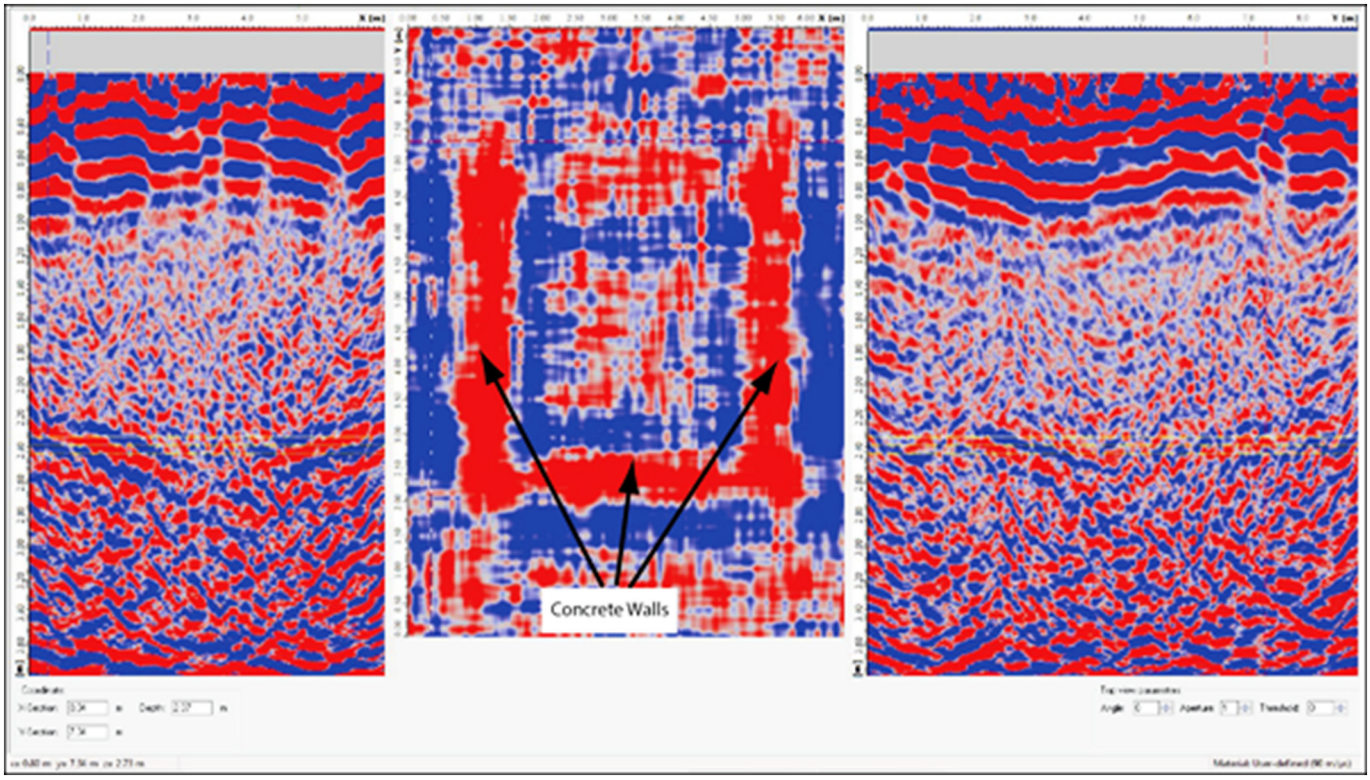

Fig. 10. The depth cut obtained because of 3-dimensional GPR measurement applied at the base of Naos.

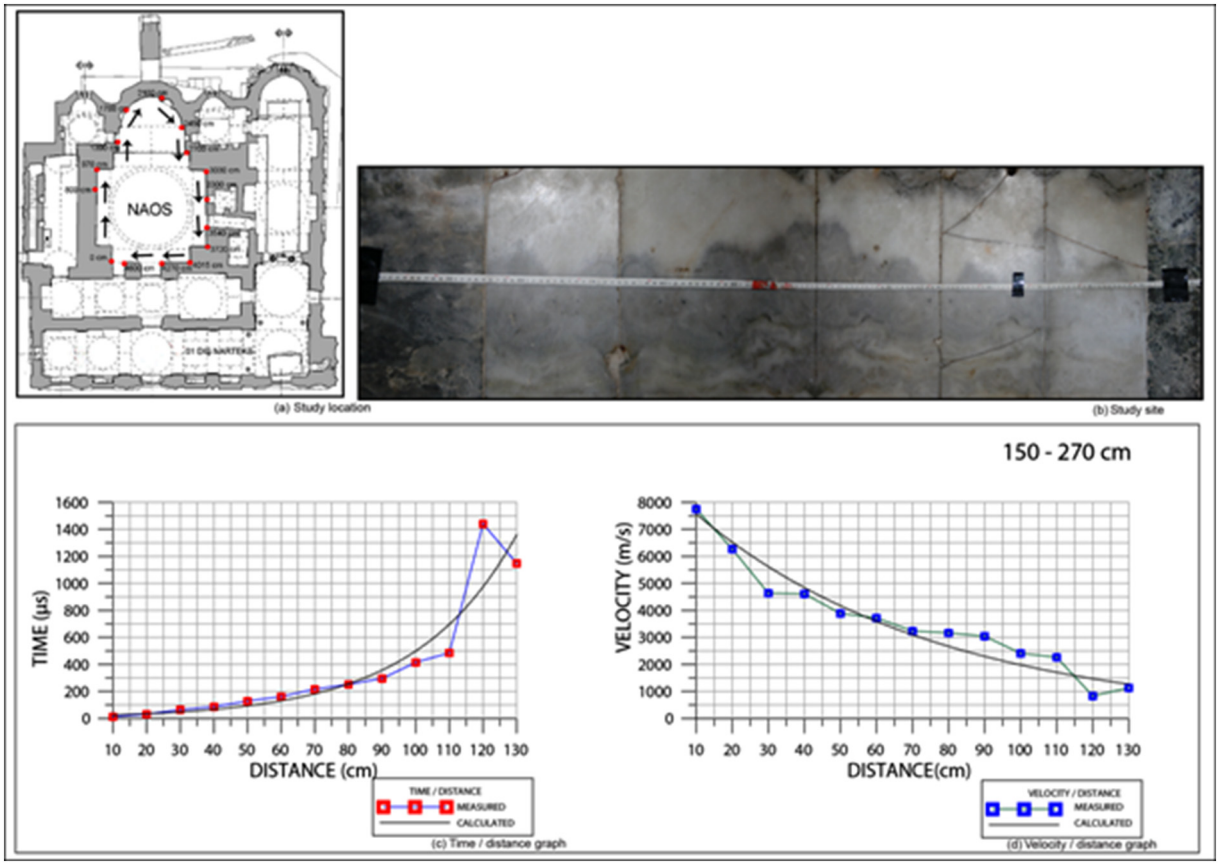

Fig. 11. 2D Graphical demonstration of UPV results.

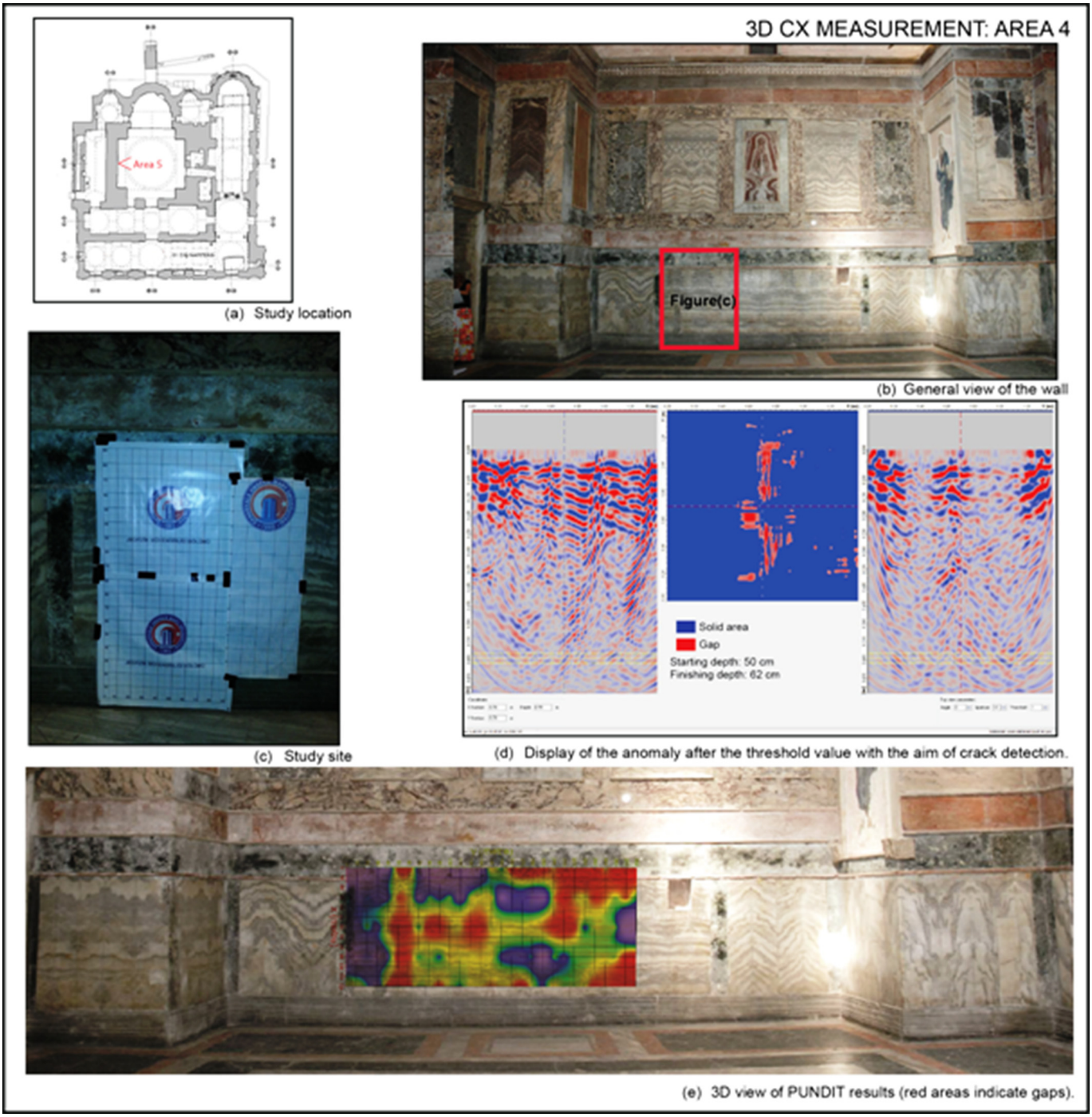

Fig. 12. An example representation of the both data results. (a) Study location (b) General view of the studied wall. (c) Detail view of the studied wall (d) GPR-CX result (red areas indicate gaps). (e) 3D view of UPV result (red areas indicate gaps). (For interpretation of the references to colour in this figure legend, the reader is referred to the web version of this article.)

The structure at the base of the naos was examined both visually and by GPR (Fig. 10) and it was understood that concrete was poured and changed. However, the size of the structure under the floor is larger than the structure that can be visually detected. It is highly probable that the entire naos base has undergone refurbishment and that the base stones were probably re-laid. This modification tracks the concrete structure defined by the red areas in Fig. 10 under the entire floor foundation. Because of the visual examination of the structure underneath the naos floor, water drops forming on the ceiling of the concrete structure were encountered. It is believed that this water is caused by the high amount of underground water present at the base of the structure. When the drainage process is carried out, this will prevent the accumulation of this water.

3.3.3. Ultrasonic Pulse Velocity (UPV) results

As a result of the UPV measurements, places on the walls of naos were identified to be cracked, voided and repaired or marble bonded points. These determinations are marked in the generated time-distance and velocity-distance graphs (Fig. 11). When the deviations from the sound wave transit speed which should be on the graphs are

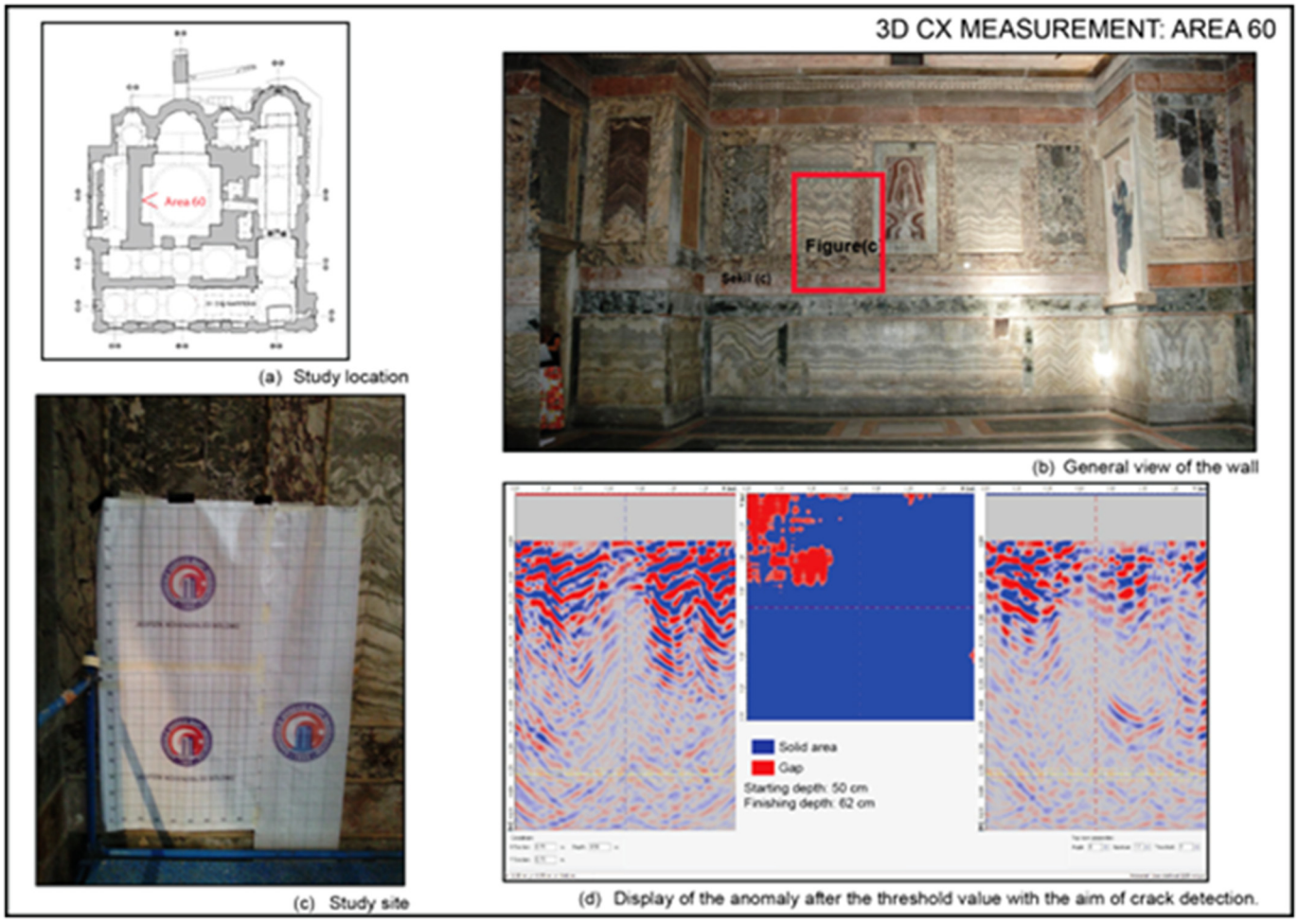

Fig. 13. An example representation of the crack structure detected at the second elevation level (the area defined as the hollow structure represents the crack plane).

Fig. 14. The top view of the cracks on the plan view and the approximate description of the crack sizes (the broken lines are below the floor and are detected in GPR floor measurements).

considered, the high-speed or short-reach paths of the waves are referred to as a tight structure and these places were repaired or are marble fixation places.

Loose wall structure, and hollow or cracked state is present in places where the speed drops and the arrival time does not lengthen. The results obtained here are also informative about the strength of the wall structure.

It was observed that the GPR was also compatible with these measurements. In addition, studies using UPV scrolling profiles also resulted in video endoscopy and results that support GPR measurements (Fig. 12a to e). The measurements were completed not only at the bottom level but also at upper levels (Fig. 13).

4. Conclusions

The application of more than one geophysical method was demonstrated to be a powerful technique to solve or diminish uncertainties associated with all indirect evaluations. In this study, two techniques were selected depending on the size of the columns and the known damage. High frequency GPR evaluation provides enough resolution to define discontinuities or changes in materials, as well as the structure shape, but results cannot be easily associated with mechanical material properties. However, the UPV technique provides less resolution, but results can reveal material information related to mechanical properties. The convergence of the problem is not always possible by applying those simplified models and sometimes unrealistic solutions are achieved. In this way, GPR data can provide sufficient and valuable information about the inner medium, allowing definition of a more accurate first model.

It was determined that the main cracks are on an axis based on measurements of high-precision GPR-CX (2.3 GHz) and UPV made on all walls within the building (Fig. 14).

The cracks on this axis were determined in the GPR profiles as having been filled during previous repairs. However, the filling material is different from the building materials (brick, joint, plaster etc.) that constitute the building walls and at the same time the presence of cavity spaces was determined. The cracks found on the axis displaying coquis shown in Fig. 14 are defined in 6 different zones according to their locations and widths. According to this;

- Cracked structure detected in the north external wall, approximate width = ~2–~6 cm.
- Cracked structures detected at the base of the internal narthex, nearly maximum width = ~6–~10 cm.
- Cracked structure detected in the wall of naos north, nearly maximum width = ~4–~8 cm.
- Cracked structure detected in the wall of south naos, approximate maximum width = ~6–~10 cm.
- Cracked structure determined on the paraclesion dome, approximate maximum width = ~10–~12 cm.
- Cracked structure detected in the south external wall, approximate maximum width = ~10–~12 cm.

Acknowledgements

We would like to thank to Directorate of the Chora Museum and ES Arc. Rest. Company for field study supports and ECAY Tech. Resc. Comp. for technical support. The authors kindest thank the anonymous referee for her/his suggestions on the manuscript.

Declaration of competing interest

There is no conflict of interest for this manuscript. We have right to use all data in the study. There is no need to get permission to publish study. The study was completed by authors of manuscript.

References

Barraca, N., Almeida, M., Varum, H., Almeida, F., Matias, M.S., 2016. A case study of the use of GPR for rehabilitation of a classified Art Deco building: the InovaDomus house. J. Appl. Geophys. 127 (1–13).

Buyuksarac, A., Isik, E., Aydın, M.C., Bektas, O., Kosaroglu, S., 2018. Non-destructive Damage Analysis for Cultural Heritage Buildings. 4th Int. Conference on Engineering and Natural Science (ICENS-2018), Book of abstracts 2018, p: 148, Kiev, Ukraine.

Chianese, D., D'Emilio, M., Di Salvia, S., Lapenna, V., Ragosta, M., Rizzo, E., 2004. Magnetic mapping, ground penetrating radar surveys and magnetic susceptibility measurements (Southern Italy). J. Archaeol. Sci. 31, 633–643.

Conyers, L.B., 2006. Ground-penetrating radar techniques to discover and map historic graves. Historical Archaeol. 40, 64–73.

Dabas, M., Camerlynck, C., Freixas, I., Camps, P., 2000. Simultaneous use of electrostatic quadrupole and GPR in urban context: investigation of the basement of the Cathedral of Girona (Catalunya, Spain). Geophysics 65 (2), 526–532.

Danniels, D.J., 2004. Ground Penetrating Radar. 2nd Ed. IET, London, UK, p. 726.

Goodman, D., 1994. Ground penetrating radar simulation in engineering and Archaeology. Geophysics 59 (2), 224–232.

Goodman, D., Nishimura, Y., Rogers, J.D., 1995. GPR time slices in archaeological prospection. Archaeol. Prospect. 2, 85–89.

Hruska, J., Fuchs, G., 1999. GPR prospection in ancient Ephesos. J. Appl. Geophys. 41, 93–312.

Kadıoğlu, S., 2003. 3D Ground Penetrating Radar-Data Acquisition, Processing, and Interpretation, 14th International Petroleum Congress and Natural Gas Congress and Exhibition of Turkey, Ankara-Turkey, Proceedings, 485–486.

Kanli, A.İ., Taller, G., Nagy, P., Tildy, P., Pronay, Z., Toros, E., 2015. GPR survey for reinforcement of historical heritage construction at fire tower of Sopron. J. Appl. Geophys. 112, 79–90.

Leckebusch, J., 2003. Ground-penetrating radar: a modern three-dimensional prospection method. Archaeol. Prospect. 10, 213–240.

Leckebusch, J., Weibel, A., Bühler, F., 2008. Semi-automatic feature extraction from GPR data. Near Surf. Geophys. 6 (2), 75–84.

Leucci, G., Negri, S., 2006. Use of ground penetrating radar to map subsurface archaeological features in an urban area. J. Archaeol. Sci. 33, 502–512.

Martinho, E., Dionísio, A., 2014. Main geophysical techniques used for non-destructive evaluation in cultural built heritage: a review. J. Geophys. Eng. 11 (5), 053001.

McCann, W.A., 1995. GPR and archaeology in central London. Archaeol. Prospect. 2, 155–166.

Ousterhout, R., 2002. The art of the Kariye Camii. London-Istanbul 2002.

Persson, K., Olofsson, B., 2004. Inside a mound: applied geophysics in archaeological prospecting at the Kings' Mounds, Gamla Uppsala, Sweden. J. Archaeol. Sci. 31, 551–562.

Piro, S., Goodman, D., Nishimura, Y., 2000. High resolution ground penetrating radar survey at Forum Novum in NovNovum e Vescovio: studying urbanism in the Tiber Valley. J. Roman Archaeol. 14, 59–79.

Sandmeier, K.J., 2003. Reflexw 4.2 Manuel Book: Sandmeier Software. Karlsruhe, Germany.

Van Millingen, A., 1912. Byzantine Churches of Constantinople. MacMillan & Co, London.

Vaughan, C.J., 1986. Ground penetrating radar surveys used in archaeological investigations. Geophysics 51, 595–604.

Yalçıner, C.Ç., 2013. Investigation of the subsurface geometry of fissure-ridge travertine with GPR, Pamukkale, western Turkey. J. Geophys. Eng. 10, 035001.

Yalçıner, C.Ç., Bano, M., Kadıoglu, M., Karabacak, V., Meghraoui, M., Altunel, E., 2009. New temple discovery at the archaeological site of Nysa (Western Turkey) using GPR method. J. Archaeol. Sci. 36, 1680–1689.

Yalçıner, C.Ç., Kurban, Y.C., Altunel, E., 2017. Research using GPR into the cause of cracks and depressions in the floor of the gallery of Hagia Sophia Museum. Constr. Build. Mater. 139, 458–466.